# A Receding Horizon Approach to Incorporate Frequency Support into the AC/DC Converters of a Multi-Terminal DC Grid

Lampros Papangelis[a], Marie-Sophie Debry[b], Patrick Panciatici[b], Thierry Van Cutsem[c,a]

[a] *Dept. of Electrical Eng. and Computer Sc., University of Liège, Belgium*
[b] *Research and Development Dept. of RTE, Versailles, France*
[c] *Fund for Scientific Research (FNRS), Belgium*

**Abstract**

This paper proposes a novel control scheme for provision of frequency support among asynchronous AC areas through HVDC grids. It is based on local controllers, each acting on a voltage source converter, using local measurements only, and supporting frequency of the adjacent AC area after a significant disturbance. The new discrete control is combined with the existing DC voltage droop technique. The formulation, inspired of Receding Horizon Control, enables providing to the AC area the desired frequency support, while at the same time taking into account various constraints, such as maintaining the DC voltage between secure operating limits. Examples obtained from a test system with a five-terminal DC network connecting two asynchronous areas demonstrate the effectiveness and robustness of the proposed control scheme in various scenarios, with emphasis on component failures.

*Keywords:* Multi-Terminal DC grid, Voltage Source Converter, frequency support, Receding Horizon Control

## 1. Introduction

In contrast to AC interconnections, most HVDC interconnected areas operate asynchronously, i.e. the various area frequencies are independent, and the speed governors of one do not respond to a frequency deviation in another. By providing the Voltage Source Converters (VSC) with dedicated controllers, Multi-Terminal Direct Current (MTDC) grids can act as "hubs" when one area is in emergency, adjusting the power transfer to that area, thus sharing the primary reserves of the various connected AC sub-systems [1].

### *1.1. Literature review and state of the art*

Frequency support to an AC area by VSCs and MTDC grids has been the subject of quite a number of publications. In the majority of them, a supplementary proportional (droop) control is added to the control structure of the VSC, enabling it to react to frequency deviations [2, 3, 4, 5]. A variant of the droop scheme was proposed in [6], where different values of droop are used depending on the severity of the disturbance. A different approach was described in [7], but it can be used for inertia emulation only and not for sharing primary reserves between asynchronous AC areas.

A number of publications are devoted to control strategies enabling primary and inertia emulation response by offshore wind farms connected to the main onshore grid through an MTDC grid [8, 9, 10, 11]. In this application, the main idea is to enable the offshore converters to change the frequency (or the AC voltage magnitude) they impose to the offshore grid [12]. This in turn triggers the controllers of the offshore wind turbines, which modify their active power production to provide inertial or primary frequency support. An alternative method based on directly communicating the onshore frequency deviation to the offshore wind farm was proposed in [13].

### *1.2. Motivation*

A drawback of the simple frequency droop control is the strong interaction with its DC voltage droop counterpart. This has been shown to reduce the efficiency of both control schemes, and adjustment of the frequency droop gain is required to achieve the desired participation to frequency support [14]. However, even this adjustment is valid only for a given configuration of the system. Namely, if one VSC is not participating to DC voltage droop control as expected, the support provided to the AC area undergoing the frequency deviation will be significantly reduced. An alternative was proposed in [15], using integral control of the power setpoint to deal with this issue.

In addition, with the exception of [13], the study of frequency support to AC areas by MTDC grids has focused on AC-side disturbances. Cases like the outage of a VSC, which could lead to significant frequency deviations,

*Email addresses:* l.papangelis@ulg.ac.be. (Lampros Papangelis), marie-sophie.debry@rte-france.com (Marie-Sophie Debry), patrick.panciatici@rte-france.com (Patrick Panciatici), t.vancutsem@ulg.ac.be (Thierry Van Cutsem)

*Authors' postprint version of a paper published in Electr. Power Syst. Res., vol. 148, pp. 1-9, Jul. 2017*

as well as severe DC voltage problems have not been investigated. In this case, a "compromise" should be sought between frequency support and maintaining an acceptable DC voltage profile of the system. Conventional control structures would require a complex set of rules and correct limits to take into account the above cases, the design of which is not obvious.

For the above reasons, a control scheme that can reliably provide the desired frequency support while being able to adapt to the system state is proposed in this paper. It is inspired of Receding Horizon Control (RHC) [16, 17]. RHC has already received attention in MTDC grids (e.g. in [18] and [19]) due to its ability to handle constraints, predict the system behavior and anticipate limit violations, which motivates its use in the present application.

The rest of the paper is organized as follows. Section 2 recalls some basics of VSC control. Section 3 details the formulation of the proposed control scheme. Section 4 reports on simulations performed on a five-terminal DC grid interconnecting two asynchronous AC areas and one offshore wind farm. Concluding remarks are offered in Section 5.

## 2. Overview of VSC control in MTDC grids and state of the art

### *2.1. DC voltage droop control*

This section recalls some basics of VSC control with emphasis on voltage droop, which interacts the most with the proposed control.

Controlling the DC voltages is of crucial concern for the correct operation of an MTDC grid. Indeed, in a DC grid, power imbalances must be rapidly corrected, given the relatively small amount of energy stored in DC capacitors. Several methods have been proposed to this purpose. The DC voltage droop technique has received significant attention [20] and has been adopted in this work. This method, inspired of AC frequency control practice, allows multiple converters to share any power imbalance in the MTDC grid while ensuring redundancy against the outage of one of them. In a droop-controlled MTDC grid some of the VSCs obey a $P$-$V$ characteristic defined by a power setpoint $P^{set}$, a voltage setpoint $V^{set}$ and a droop $K_V$. In steady state the VSC power $P$ is linked to the DC voltage $V$ through:

$$P = P^{set} - K_V(V - V^{set}) \tag{1}$$

where a positive power corresponds to rectifier operation. Therefore, following a power deficit in the MTDC grid, the DC voltage will start decreasing and the VSC will increase the power it injects into the DC grid until the balance is restored.

A simplified diagram of the VSC control structure based on the work in [20] is shown in Fig. 1, including the DC voltage droop control. The diagram focuses on the outer control loops which consist of the active and reactive power control. The former varies according to the DC voltage of the VSC as described by Eq. (1). The reactive power control is also shown in Fig. 1 for completeness purposes. In this mode the reactive power $Q$ is assumed to be controlled to its $Q^{set}$ value. These control loops provide the active and reactive power commands ($P^{cmd}$ and $Q^{cmd}$, respectively) to the current controller which then adjusts the modulation logic of the VSC. A Phase Lock Loop (PLL) is usually used to synchronize the VSC to the AC grid.

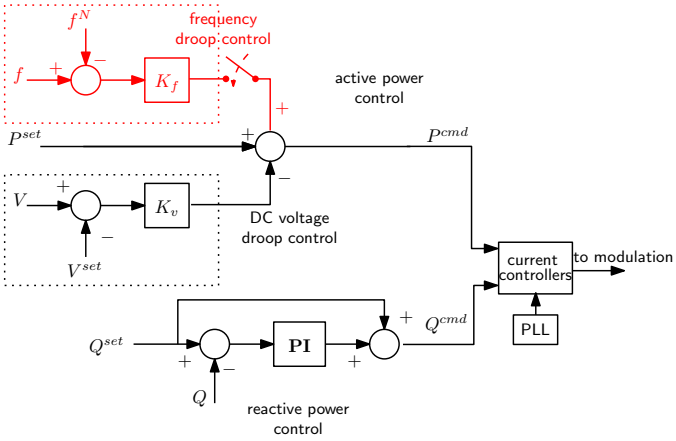


Figure 1: Simplified diagram of the VSC control structure

### *2.2. Frequency droop control*

As already mentioned in the Introduction, the most widespread implementation for frequency support consists of adding a supplementary droop term in the control structure of the VSC as shown in Fig. 1. With this addition the power of the VSC in steady-state is equal to:

$$P = P^{set} - K_V\,(V - V^{set}) + K_f\,(f - f_N) \tag{2}$$

where $K_f$ the chosen frequency droop, $f$ the AC system frequency and $f_N$ the nominal frequency.

## 3. Proposed frequency control

### *3.1. Requested features of the control*

Some works have investigated the possibility to use the MTDC grid in order to "reach a frequency consensus" between the interconnected asynchronous AC areas [21, 22], i.e. eventually bring all frequencies to the same value. This is not the track followed in this work, whose aim is to consider frequency support as an "emergency" control scheme, as also suggested in [23]. Therefore, for small frequency deviations the frequency support scheme remains inactive. This also serves the purpose of preventing continuous interactions between the frequency controls of AC systems which were otherwise planned to operate asynchronously. On the other hand, in response to a large enough frequency deviation in one AC area, the VSCs connected to the latter sense the frequency deviation and correspondingly adjust

the power transfer through the MTDC grid, thus taking advantage of the primary reserves of other AC areas.

The participating VSC is controlled to provide in steady state a pre-defined fraction of the total power injection needed to support the frequency in the AC area of concern, as for a power plant under speed governor control. This can be achieved by changing the power setpoint $P^{set}$ of the $P$-$V$ characteristic (1) until the above objective is satisfied. As pointed out in [15], in order a VSC in frequency droop mode to achieve the desired power participation, some kind of integral action is required so that the total change of its power setpoint counteracts the impact of the resulting DC voltage deviation on its power flow (according to Eq. (1)).

Clearly, the added control should not jeopardize the operation of the MTDC grid as well the other AC areas. This imposes to obey constraints on the DC voltage, on the rate of change of powers, etc. Furthermore, a concern which, to the authors' knowledge, has not received proper attention is the controller behavior when the other AC areas do not "cooperate" as expected, e.g. when the VSCs of one area do not participate as expected in DC voltage control and, hence, do not provide the power requested by the frequency controlling VSCs.

Finally, it is highly desirable to rely only on local measurements readily available to each VSC. By so doing, fast and reliable performance can be achieved without resorting to communication between converters, which can be subject to delays and failures.

### *3.2. Brief recall of RHC principle*

For reasons presented in the Introduction, the proposed control relies on the RHC concept also referred to as Model Predictive Control. This multi-step, optimization-based control scheme consists of computing a sequence of control changes which minimizes an objective and satisfies constraints in the future [16]. This optimization relies on a model of the future system evolution. In this work, the above model is static, which is justified by the speed of action of power electronics and VSC controls, compared to the sampling period of the discrete controller (in the order of half a second).

The RHC control logic can be summarized as follows. At the current discrete time $k$, the controller has received the latest available measurements and computes optimal control actions $(\Delta\mathbf{u}(k), \ldots, \Delta\mathbf{u}(k+N_c-1))$ that have to be applied from $k$ up to the end of the control horizon $k+N_c-1$, so that the system meets a desired target at the end of the prediction horizon $k+N_p$ ($N_p \geq N_c$). Out of this sequence, only the first component $\Delta\mathbf{u}(k)$ is applied. Then, at the next time instant $k+1$, the procedure is repeated for the updated control and prediction horizons, using the newly received measurements.

### *3.3. Constrained optimization problem*

The proposed controller bears the spirit of an "emergency" scheme, thus being inactive in normal operation.

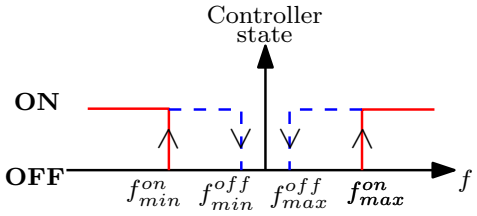


Figure 2: Controller activation logic

Its activation is triggered by frequency deviation. As shown in Fig. 2, as long as frequency stays inside a pre-specified range $[f^{on}_{min}, f^{on}_{max}]$, the controller remains idle (OFF state), while it is activated as soon as frequency leaves the deadband (ON state). Once the controller has been activated, it remains active until the frequency is restored inside a narrower range $\left[f^{off}_{min}, f^{off}_{max}\right]$.

Let $t^\star$ be the time when the control is activated, and $P$ the power injected by the VSC into the MTDC grid.

The main objective of frequency control is to adjust $P$ so that the steady-state participation of the VSC is proportional to the frequency deviation, i.e.

$$\lim_{t\to\infty} \left[\, P(t) - P(t^\star) - K_f \left(f(t) - f_N\right)\right] = 0. \tag{3}$$

The measurements used at time $k$ are:

$P^m(k)$ : the power flowing through the converter
$V^m(k)$ : the voltage at its DC bus
$f^m(k)$ : the frequency at its AC bus.

These measurements are readily available in the converter sub-station. Specifically, AC frequency is measured through the PLL. Note that multiple VSCs supporting the same AC area will not measure exactly the same frequency, since the local measurements may be impacted by the initial disturbance and by the resulting electromechanical oscillations.

A reference evolution (or "trajectory" [17]) is defined with the objective of bringing the VSC power from its currently measured value to a value satisfying Eq. (3) in a finite number $N_c$ of control steps: for $j = 1, \ldots, N_c$:

$$\begin{aligned} &P^{ref}(k+j) = \\ &P^m(k) + \frac{j}{N_c}\left[\, P(t^\star) + K_f(f^m(k) - f_N) - P^m(k)\right]. \end{aligned} \tag{4}$$

It is easily checked by setting $j = N_c$, that the reference power at the end of the control horizon satisfies the participation defined by Eq. (3), if the frequency was already at its final value. This point is further discussed at the end of this sub-section.

The constrained optimization at the heart of the proposed control consists in minimizing the deviations with respect to the above reference values:

$$\min_{V,P,\epsilon,\Delta P^{set}} \sum_{j=1}^{N_c} [P^{ref}(k+j) - P(k+j)]^2 + v \sum_{j=1}^{N_c} [\epsilon(k+j)]^2 \tag{5}$$

subject to the following constraints: for $j = 1, \ldots, N_c$:

$$V^{low}(k+j) - \epsilon(k+j) \leq V(k+j) \leq V^{up}(k+j) + \epsilon(k+j) \quad (6)$$

$$\epsilon(k+j) \geq 0 \quad (7)$$

$$P^{min} \leq P(k+j) \leq P^{max} \quad (8)$$

$$V(k+j) = V(k+j-1) + s_v \, \Delta P^{set}(k+j-1) \quad (9)$$

$$\begin{aligned} P(k+j) = P(k+j-1) + \Delta P^{set}(k+j-1) \\ - K_v \left( V(k+j) - V(k+j-1) \right) \end{aligned} \quad (10)$$

where $\Delta P^{set}$ is the change of VSC power setpoint, $\epsilon$ a slack variable, and $v$ a weight penalizing voltage violations.

Inequality (6) specifies that the DC voltage should not exceed the limits $V^{low}$ and $V^{up}$. In case the optimization problem becomes infeasible, these constraints are relaxed, with the $\epsilon$ variables taking nonzero values. The constraint violation is, however, kept as small as possible by setting the weight $v$ to a high value. Note that $V^{low}$ and $V^{up}$ evolve with time $k+j$ in order to bring the voltage progressively inside a desired range defined by the minimum and maximum security limits $V^{min}$ and $V^{max}$. This is further detailed in sub-section 3.5.

Constraint (8) imposes the VSC power to stay within limits.

Equations (9) and (10) make up the prediction model, initialized by setting the voltage (resp. power) to the last available measurement, i.e. $V(k) = V^m(k)$ (resp. $P(k) = P^m(k)$). The prediction horizon is taken equal to the control horizon $N_c$. $s_v$ is the sensitivity of the DC voltage of a given VSC to the setpoint change $\Delta P^{set}$ of the same VSC. Its computation is explained in the next sub-section.

The formulation can accommodate other constraints, such as maximum rate of change of power and/or DC voltage, maximum steady-state participation to frequency control, etc.

A model of frequency dynamics could be also included in the formulation, more precisely to predict the future frequency values and use them in Eq. (4). This would require a simplified model of the AC system, providing the frequency response to the $\Delta P^{set}$ power changes. However, such a model may not be available or accurate, and it has not been considered in this work. Instead, in Eq. (4), the future frequency values are set to the latest measurement $f^m(k)$, updated at each time step. Extensive tests have shown that this approximation is properly compensated by the closed-loop RHC scheme, as demonstrated in Section 4.

### *3.4. Determination of the sensitivity $s_v$*

In an MTDC grid consisting of $n$ converters, the relation between the DC voltage changes and the VSC power setpoint changes was derived in [24] and can be written as:

$$\Delta \boldsymbol{P}^{set} = \boldsymbol{S}_p \, \Delta \boldsymbol{V} \quad \text{or} \quad \Delta \boldsymbol{V} = \boldsymbol{S}_v \, \Delta \boldsymbol{P}^{set} \quad (11)$$

$$\text{where:} \quad \boldsymbol{S}_p = \boldsymbol{S}_v^{-1} = \boldsymbol{J}_{dc} + \mathbf{diag}(K_{v1} \ldots K_{vc}). \quad (12)$$

$\boldsymbol{J}_{dc}$ is the $(n \times n)$ Jacobian matrix of DC power flows with respect to DC voltages, and $\mathbf{diag}(K_{v1} \ldots K_{vn})$ a diagonal matrix with the voltage droops (see Eq. (1)) of all VSCs as diagonal entries.

If it is assumed that an AC area can be connected to the MTDC grid through more than one VSC, it is possible that a frequency excursion in that area activates frequency control in more than one terminals. If the $c$-th terminal is one of them, its DC voltage varies under the combined effect of several power changes as follows:

$$\Delta V_c = \sum_{i \in \mathcal{A}} [\boldsymbol{S}_v]_{ci} \, \Delta P_i^{set} \quad (13)$$

where $\mathcal{A}$ denotes the set of activated terminals. In order to control each of them independently of the others, an approximate scalar sensitivity $s_v$ is sought. It can be obtained under the following reasonable approximations:

a. The controllers of all terminals connected to the same area have the same parameters (in particular the same sampling period);
b. the control action calculated by each controller at each time step is proportional to the corresponding frequency droops $K_f$ (see Eq. (4)), i.e.

$$\forall i, c \in \mathcal{A}: \quad \frac{\Delta P_i^{set}}{K_{f,i}} \approx \frac{\Delta P_c^{set}}{K_{f,c}}. \quad (14)$$

From Eq. (14), the various power changes can be expressed in terms of the $c$-th one:

$$\Delta P_i^{set} = \frac{K_{f,i}}{K_{f,c}} \Delta P_c^{set} \quad (15)$$

Substituting this result in (13) yields:

$$\Delta V_c = \sum_{i \in \mathcal{A}} [\boldsymbol{S}_v]_{ci} \, \frac{K_{f,i}}{K_{f,c}} \Delta P_c^{set} \quad (16)$$

from which the sensitivity is obtained as:

$$s_v = \sum_{i \in \mathcal{A}} [\boldsymbol{S}_v]_{ci} \, \frac{K_{f,i}}{K_{f,c}}. \quad (17)$$

This sensitivity accounts for the effect on DC voltages of all the VSCs supporting the frequency of an area. Note that no information is exchanged between terminals in the course of controlling frequency. In addition, the sensitivities (17) need not be updated often, but only after a topological change in the MTDC grid. In fact, the approximations embedded in Eq. (17) are corrected by the closed-loop RHC scheme.

### *3.5. Treatment of limits violations*

In normal operation, the DC voltage of the VSC is between the minimum and maximum limits $V^{min}$ and $V^{max}$, respectively. In this case, the bounds in constraint (6) are: for $j = 1, \ldots, N_c$:

$$V^{low}(k+j) = V^{min}, \quad V^{up}(k+j) = V^{max} \quad (18)$$

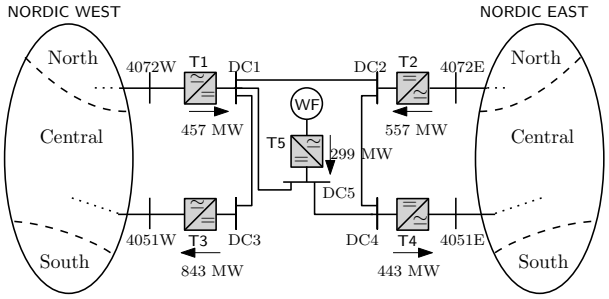


Figure 3: Test system topology and initial power flow

However, it is possible that after a disturbance or due to the frequency support, the DC voltage of the VSC temporarily exceeds its normal operating limits. To avoid abrupt corrections the relevant bound is progressively tightened, starting from the measurement value, as follows: for $j = 1, \ldots, N_c$:

$$V^{low}(k+j) = V^m(k) + \left(V^{min} - V^m(k)\right) \frac{j}{N_c} \qquad (19)$$

$$V^{up}(k+j) = V^m(k) + \left(V^{max} - V^m(k)\right) \frac{j}{N_c}. \qquad (20)$$

It is easily checked by setting $j = N_c$ in Eqs. (19) and (20) that the value of the limits at the end of the control horizon are the specified security values $V^{min}$ and $V^{max}$.

## 4. Simulation results

### *4.1. Test system and modeling*

The proposed control scheme has been tested on a system consisting of two asynchronous AC areas and one offshore wind farm, connected through a five-terminal MTDC grid, as sketched in Fig. 3.

Each AC area is based on the so-called Nordic test system, set up by an IEEE Task Force and detailed in [25], to which the reader is referred for a more detailed description. In both replicas, generator g20, which represented a large external AC system has been removed and the nearby equivalent load has been accordingly adjusted. Each subsystem has two points of connection to the MTDC grid, in the North and the Central areas, respectively.

All generators are represented with their automatic voltage regulators, excitation systems, speed governors and turbines as detailed in [25]. Each VSC is modeled in some detail with 28 differential-algebraic equations involving the phase reactor and DC capacitor dynamics, inner and outer control loops, PLLs, filters, etc. The DC branches are represented only by their series resistance by neglecting the series inductance and accounting for their DC capacitances in the terminal capacitors [15]. T5 is assumed to impose constant frequency and voltage on its AC side, thus acting as a slack bus for the offshore wind farm, merely modeled as a power injection.

Among the five VSCs, all but T5 operate in DC voltage droop mode with $K_v = 5$ pu (on the VSC nominal power base), and can be equipped with the proposed frequency control with a gain $K_f = 20$ pu. A deadband of $\pm 200$ mHz is used for the activation of the controller and of $\pm 10$ mHz for deactivation (see Fig. 2). The initial power in each VSC is shown in Fig. 3.

All discrete controllers have a sampling time $T = 0.5$ s, which is long compared to the time constants of power electronics but short with respect to frequency dynamics. In order to synchronize the VSCs acting on the same AC area, the controls $\Delta P^{set}$ are applied at discrete times $kT$ ($k = 1, 2, \ldots$), assuming that each controller is relying on a GPS-synchronized clock. Each VSC collects the measurements $P^m(k), V^m(k)$ and $f^m(k)$ at times $kT - 0.1\,s$ ($k = 1, 2, \ldots$) to account for the time needed to solve the optimization problem.

The control and prediction horizons have been set both to $N_c = 3$ to obtain a short enough time response. The weighting factor $v$ (see Eq. (5)) has been chosen to $10^4$.

The active power limits of each VSC have been set equal to the VSC nominal active power of 1000 MW, i.e. $P^{min} = -10$ and $P^{max} = +10$ pu on a 100 MW base . The voltage limits at the DC buses of T1 - T4 have been chosen equal to $V^{min} = V^o - 0.05$ and $V^{max} = V^o + 0.05$ pu, where $V^o$ is the initial DC voltage. The nominal DC voltage of all VSCs is $\pm 320$ kV.

All time simulations were performed in phasor mode with RAMSES, a time simulation software developed at the University of Liège [26], using the techniques described in [27]. A total of five scenarios are demonstrated. The first two concern an AC-side disturbance, for which a comparison between the proposed controller and the conventional frequency droop scheme is performed. The last three scenarios show the performance of the proposed scheme in a more intricate case, initiated by a DC-side disturbance.

### *4.2. Disturbance in the AC system*

The first two scenarios correspond to the tripping of generator g8E in the East subsystem, which activates frequency control by T2 and T4.

A comparison is conducted with the conventional frequency droop control (see Fig. 1) using the same droop $K_f$. To facilitate the comparison, the droop control is also implemented as a discrete controller with the same sampling time as the RHC-based control ($T = 0.5$ s).

#### *4.2.1. Scenario 1*

Figure 4a shows the frequencies in both AC areas, with and without frequency support by T2 and T4. As expected, the activation of frequency support by T2 and T4 leads to a less pronounced frequency dip, and a higher final frequency value, to the expense of a frequency deviation in the West subsystem, although milder. However, it can be seen that the proposed control provides more power than the conventional droop. The reason is the enforcement of the desired steady-state participation according to Eq. (3), in contrast to the conventional frequency droop control.

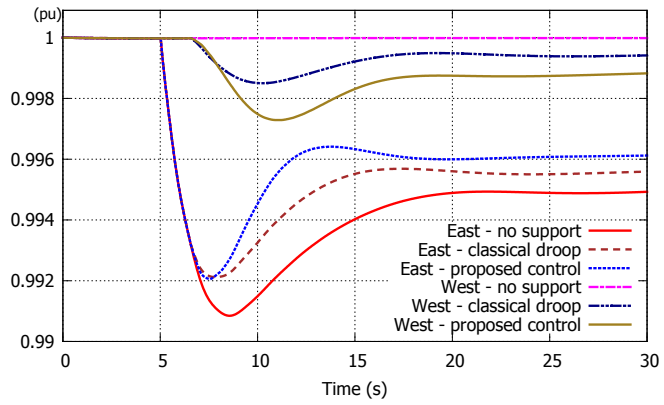


(a) AC system frequencies

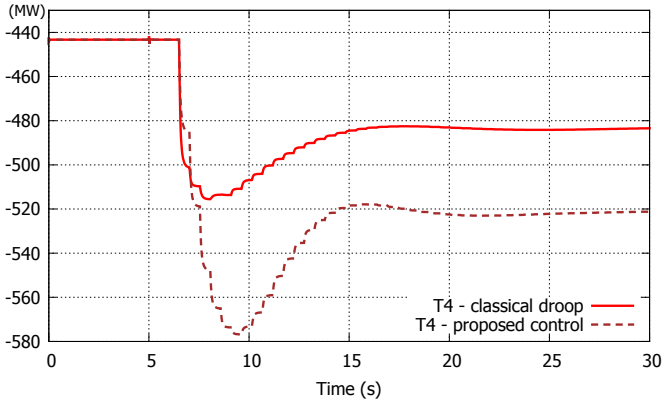


(b) DC power of T4

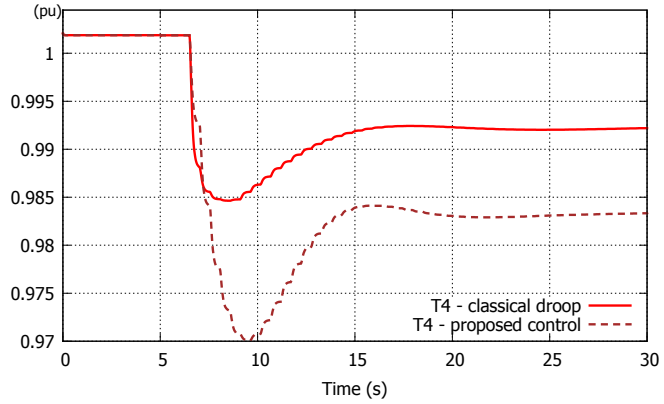


(c) DC voltage at bus DC4

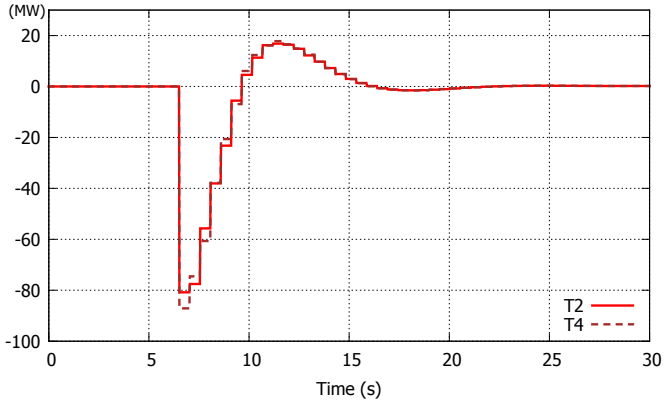


(d) Control steps $\Delta P^{set}$ in T2 and T4

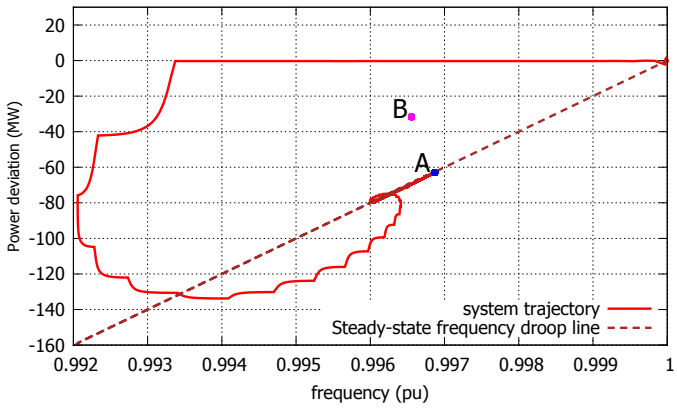


(e) Power deviation vs frequency for T4

Figure 4: Scenario 1: simulation results

This is further illustrated in Fig. 4b, which shows the DC power of T4 for both schemes. It is noted that frequency control is activated at $t = 6$ s and, hence, the first control action is applied at $t = 6.5$ s in both cases. The RHC-based scheme provides the correct participation in steady state compared to the conventional droop scheme whose effect is partially counteracted by the DC voltage droop control. T2 presents a similar response.

The DC voltage at bus DC4 is shown in Fig. 4c. The other DC voltages experience similar variations. Clearly, by enforcing the required participation through the RHC control, the DC voltages of the grid experience larger deviations. However, this is acceptable as long as these deviations are kept between standard operating limits.

The control steps ($\Delta P^{set}$) of the proposed controller are shown in Fig. 4d for both T2 and T4.

It must be highlighted that the time response of the proposed frequency control is comparable to the one of conventional power plants. This is important in order to limit the impact of the initial disturbance on the West system. Indeed, if faster response was provided (as made possible by power electronics), the West system might ex-

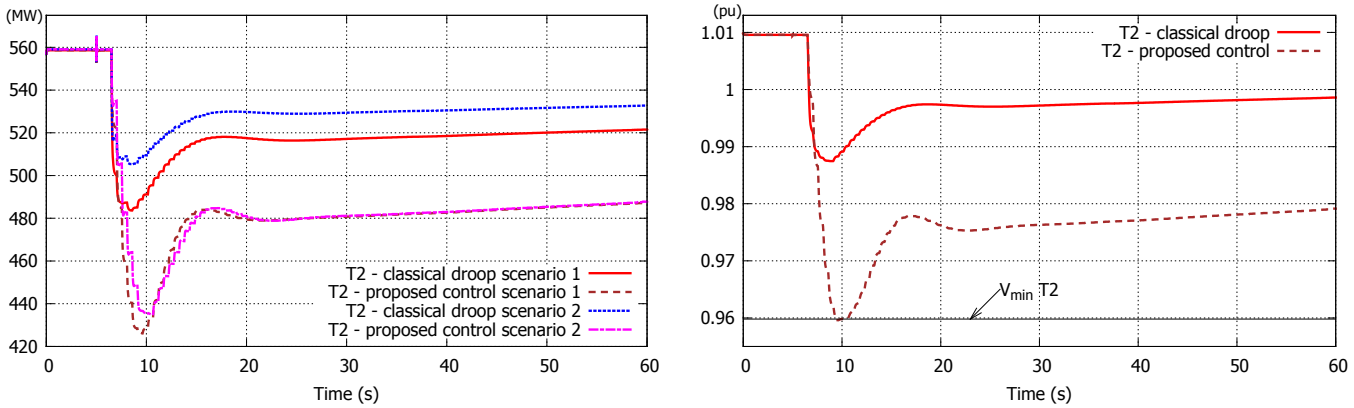


(a) DC power of T2

(b) DC voltage at bus DC2

Figure 5: Scenario 2: simulation results

perience a larger frequency drop.

Finally, Fig. 4e shows the power deviation $P(t) - P(t^\star)$ vs frequency change $f - f_N$ plot for T4, superimposed to the dotted line which corresponds to the desired steady-state participation $K_f\,(f - f_N)$. Before frequency control activation, the T4 power does not deviate significantly from its initial value (see horizontal upper part of the trajectory), whereas after its activation, it eventually converges to point A on the frequency droop line, confirming that (3) is satisfied. Point B corresponds to the steady state reached with the conventional droop scheme.

#### *4.2.2. Scenario 2*

The purpose of this scenario is to demonstrate the safe RHC scheme behavior in case of unexpected non-cooperation between the two areas.

It involves the same initial generator outage, but now T3 does not participate in DC voltage control as expected. Specifically, it is assumed that T3 is operating in constant power mode ($K_v = 0$). This could be the result of a non-reported action by the transmission system operator of the West system, due to stressed conditions in that system. It must be emphasized that the sensitivity $s_v$ has not been updated to account for this "hidden failure".

After the tripping of g8E, frequency support is activated in T2 and T4 as in the previous scenario. However, the whole power requested by T2 and T4 is now provided by T1 alone. Indicatively, the DC power of T2 is shown in Fig. 5a. The power of T2 in scenario 1 is repeated for comparison. It can be seen that with the conventional control, T2 provides even less support than in scenario 1. The reason is the larger DC voltage deviation, due to the non-participation of T3, which further reduces the frequency support by T2 and T4. On the other hand, the proposed controller, eventually provides the same participation as in scenario 1, in spited of the T3 failure.

The DC voltage at bus DC2 is shown in Fig. 5b. It can be seen that the proposed RHC-based control leads to a larger DC voltage deviation since it requires a larger change of the power setpoint of T2 in order to satisfy the desired participation. However, when the lower limit is approached, the controller automatically adapts its behavior to avoid further DC voltage degradation. Following the recovery of the East system frequency, the controller removes some of the power it had to inject in the AC system and the DC voltage recovers, and settles inside the allowed operating zone.

### *4.3. Disturbance in the MTDC system*

The following scenarios deal with a disturbance in the MTDC system, i.e. the tripping of terminal T3 at $t = 3$ s. In all cases, this event is followed by a very fast power adjustment of T1, T2 and T4, under the effect of DC voltage droop control. The outage is expected to cause a significant frequency deviation in both AC systems, but in opposite directions, as already quoted in [13] and [24]. Indeed, since the West system is missing the 843 MW injected by T3, it will experience under-frequency. The East system, on the other hand, will experience over-frequency. Each of the following scenarios relates to a different outcome:

a. Scenario 3: only T1 is equipped with the proposed RHC control.
b. Scenario 4: only T2 and T4 are equipped with that control.
c. Scenario 5: all remaining terminals (T1, T2 and T4) are equipped with that control.

#### *4.3.1. Scenario 3*

When frequency support is activated in T1 only, the system evolves as shown in Figs. 6a-6c.

Figure 6a shows the frequencies of both systems with and without frequency support by T1. It can be seen that the frequency support activation slightly improves the response in both AC areas.

The DC powers of the VSCs are shown in Fig. 6b. Due to DC voltage droop control, the powers of T1, T2 and T4 change rapidly to restore the power balance of the MTDC grid. Then, at $t = 6.5$ s, frequency support is activated in T1. At this point, the choice of the correct reference

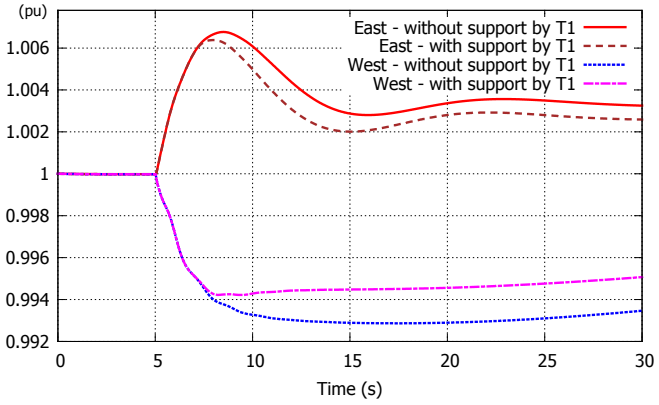


(a) AC system frequencies

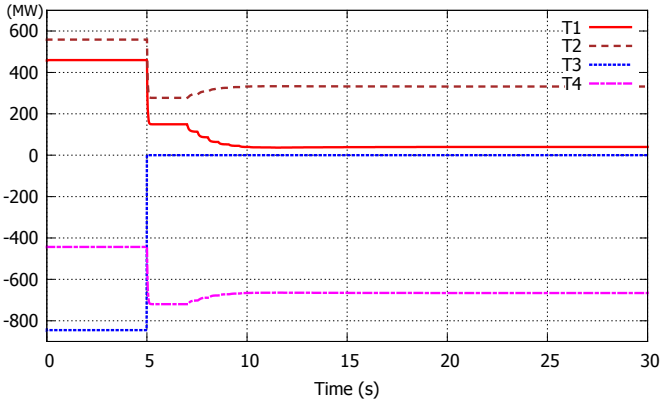


(b) DC power of VSCs

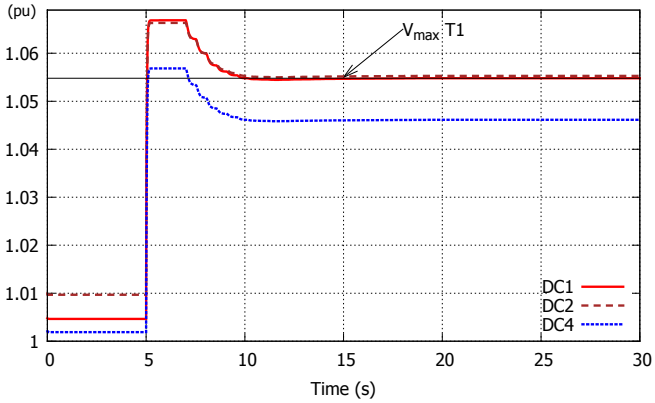


(c) MTDC grid voltages

Figure 6: Scenario 3: simulation results

value $P(t^\star)$ has to be stressed. This value should be taken after the VSC power has settled under the effect of the DC voltage droop control. Otherwise, the VSC will not provide the desired participation that corresponds to the new configuration of the system. Given that the DC voltage response is much faster than the AC frequency response, it can be assumed that the MTDC grid will have reached a steady state before the frequency of the AC network exceeds the specified deadband. For this reason, it has been chosen to set $P(t^\star)$ to the last power measurement taken before the controller activation.

Finally, the DC voltages at buses DC1, DC2 and DC4 are shown in Fig. 6c. Following the tripping of T3 they all rise very fast but are promptly stabilized by the DC voltage droop control. However, the DC voltage of T1 settles outside its limit. Therefore, following the activation of frequency support, the controller not only pursues to change the power of T1 in order to satisfy the desired participation, but also to bring the DC voltage below the maximum limit. Indeed, the voltage at bus DC1 eventually settles on its upper limit.

It fact, in this case the proposed controller automatically provides more power than the one specified by the desired droop gain. The reason is that the change of the T1 power setpoint required in order to bring the DC voltage to its limit is greater than the one required to satisfy the desired participation to frequency support. This behavior is beneficial, since providing more power to the West system favors the response of the whole combined AC/DC system, i.e. it improves the frequency response of both East and West subsystems and the DC voltages in the DC grid. It should be also noted that if the opposite was true, i.e. the change of power setpoint required to satisfy the desired frequency participation was greater than the one needed to bring the DC voltage to its limit, the controller would eventually provide the desired participation and the DC voltage would settle inside its desired operating range. Therefore, it can be concluded that in this case the proposed scheme will provide at least the desired participation.

### *4.3.2. Scenario 4*

Figures 7a-7c show the evolution of the system when T2 and T4 are equipped with the proposed controller instead of T1. As in scenario 3, following the tripping of T3, DC voltages are promptly stabilized by the DC voltage droop control as shown in Fig. 7a.

However, following the activation of frequency support by T2 and T4 at $t = 6.5$ s, the controllers do not try to support the frequency of East system by increasing their injection to the DC system, because this would further increase the DC voltage violation. Instead, as shown in

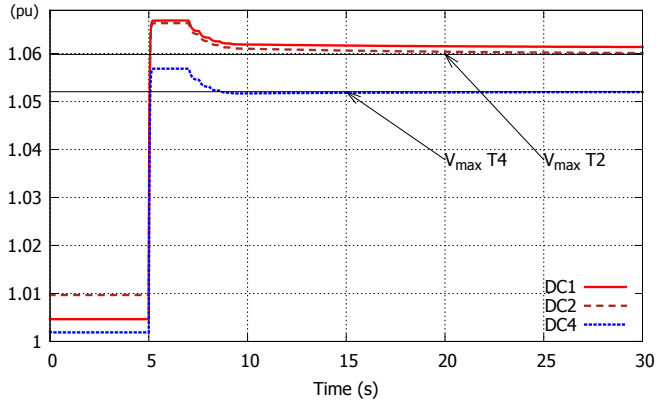


(a) MTDC grid voltages

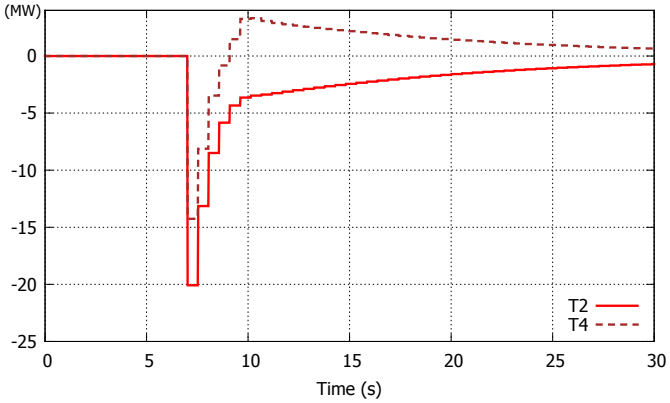


(b) Control steps $\Delta P^{set}$ in T2 and T4

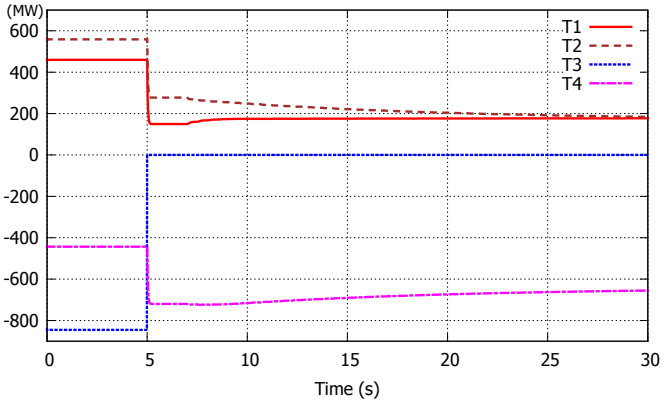


(c) DC power of VSCs

Figure 7: Scenario 4: simulation results

Fig. 7b, they act in the opposite direction and successfully bring their DC voltages (shown in Fig. 7a) below their limits.

Figure 7c reveals a slow shift of power from T2 to T4. This is because the DC voltage of T4 is restored a little below its limit before the DC voltage of T2 is also corrected. Therefore, since no communication between the VSCs has been assumed, the controller of T4 identifies that it could inject some power in the DC grid. On the other hand, since T2 keeps its DC voltage at the requested limit, it modifies its power setpoint to cover for the power change of T4. Eventually, this power shift stops when both DC voltages are at their limits.

It should be highlighted that if the initial disturbance was not severe enough to cause the DC voltage violation, the frequency controllers would behave as expected, i.e. they would draw power from the East subsystem to mitigate the frequency increase.

### *4.3.3. Scenario 5*

In this last scenario, all T1, T2 and T4 are provided with the proposed frequency control scheme. Thus, at $t = 6.5$ s, the three VSCs start adjusting their power setpoints, first to restore their DC voltages below their limit, as in scenarios 3 and 4, then to satisfy their desired participation to frequency support. Thus, initially, all VSCs decrease their injection in the DC grid to correct the DC voltages. This is achieved at approximately $t = 7.5$ s. Since all DC voltages are restored below their limits, the actions of all controllers are towards satisfying the desired participation to frequency support.

As previously, T1 decreases its DC power injection, as shown in Fig. 8a. On the contrary, since the East system experiences over-frequency, T2 and T4 attempt to increase their DC injections. This leads to again increasing the DC voltages of the system, as shown in Fig. 8b, with the outcome that the maximum DC voltage constraint of T1 becomes active. At the same time, since the DC voltages of T2 and T4 have not reached their limits, they keep changing their power output in order to satisfy their own participation to frequency control of the East system, as shown in Fig. 8a.

Eventually, the system reaches a steady state when the desired participation of T2 and T4 has been satisfied, whereas T1 is operating at its maximum DC voltage limit. It is also noted that eventually T1 provides more power to the West subsystem than specified by its droop gain. As in scenario 3, this is beneficial since a larger part of the pre-disturbance power exchange between the two areas is restored.

This severe scenario was aimed at demonstrating the ability to preserve DC grid operation even when all VSCs

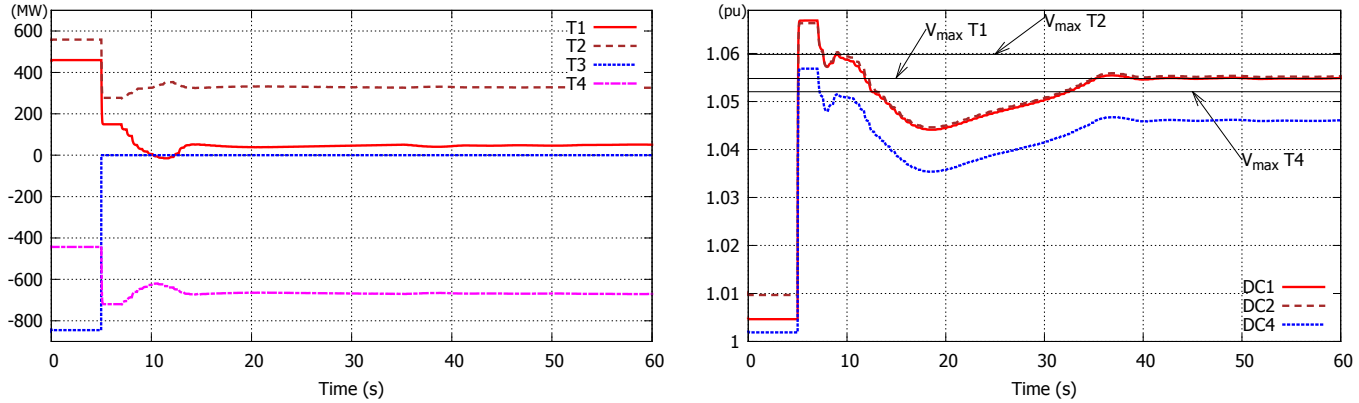


(a) DC power of VSCs

(b) MTDC grid voltages

Figure 8: Scenario 5: simulation results

switch to frequency support control mode. Clearly, this situation arises since no communication is utilized and all VSCs aim at supporting frequency. However, the system could be reset (by a slow, centralized controller or action) in order to restore the DC voltage near its nominal value, resume normal operation and restore the whole power transfer between the two areas.

## 5. Conclusion

This paper has presented a novel control scheme for primary frequency support among asynchronous AC areas through MTDC grids. The proposed control relies on a receding horizon, multi-time step, constrained optimization-based scheme, which allows to explicitly take into account various MTDC grid constraints, such as DC voltage limits. In addition, it relies on local measurements only, i.e. no communication is needed between the various AC/DC terminals.

The reported simulation results have demonstrated the capability of the proposed scheme to take appropriate actions to support the frequency of the adjacent system while keeping its DC voltage in a specified range of values. It was shown that the system remains stable and between limits in case of unexpected non-cooperation of some terminals or when frequency support is activated in all of them. Emphasis has been put on scenarios involving the tripping of a VSC, instead of a generator, which require different treatment.

The work is currently extended to the coordination of the proposed control scheme with a centralized, slower control of the MTDC grid, aiming at monitoring the whole HVDC grid and coordinating the VSCs, as well as with the secondary frequency control in the adjacent AC areas.

## References


[1] D. Van Hertem, R. H. Renner, Ancillary services in electric power systems with HVDC grids, IET Generation, Transmission & Distribution 9 (2015) 1179–1185.

[2] T. M. Haileselassie, K. Uhlen, Primary frequency control of remote grids connected by multi-terminal HVDC, in: Proc. 2010 IEEE PES General Meeting.

[3] N. R. Chaudhuri, R. Majumder, B. Chaudhuri, System Frequency Support Through Multi-Terminal DC (MTDC) Grids, IEEE Transactions on Power Systems 28 (2013) 347–356.

[4] R. Wiget, G. Andersson, M. Andreasson, D. V. Dimarogonas, K. H. Johansson, Dynamic simulation of a combined AC and MTDC grid with decentralized controllers to share primary frequency control reserves, in: Proc. 2015 IEEE PES Eindhoven PowerTech.

[5] C. E. Spallarossa, Y. Pipelzadeh, T. C. Green, Influence of frequency-droop supplementary control on disturbance propagation through VSC HVDC links, in: Proc. 2013 IEEE PES General Meeting.

[6] T. K. Vrana, L. Zeni, O. B. Fosso, Active power control with undead-band voltage & frequency droop applied to a meshed DC grid test system, in: Proc. 2012 IEEE ENERGYCON.

[7] J. Zhu, C. D. Booth, G. P. Adam, A. J. Roscoe, C. G. Bright, Inertia Emulation Control Strategy for VSC-HVDC Transmission Systems, IEEE Transactions on Power Systems 28 (2013) 1277–1287.

[8] Y. Phulpin, Communication-Free Inertia and Frequency Control for Wind Generators Connected by an HVDC-Link, IEEE Transactions on Power Systems 27 (2012) 1136–1137.

[9] Y. Pipelzadeh, B. Chaudhuri, T. C. Green, Inertial response from remote offshore wind farms connected through VSC-HVDC links: A Communication-less scheme, in: Proc. 2012 IEEE PES General Meeting.

[10] S. I. Nanou, G. N. Patsakis, S. A. Papathanassiou, Assessment of communication-independent grid code compatibility solutions for VSC–HVDC connected offshore wind farms, Electric Power Systems Research 121 (2015) 38–51.

[11] B. Silva, C. L. Moreira, L. Seca, Y. Phulpin, J. a. Pecas Lopes, Provision of Inertial and Primary Frequency Control Services Using Offshore Multiterminal HVDC Networks, IEEE Transactions on Sustainable Energy 3 (2012) 800–808.

[12] C. Feltes, I. Erlich, Variable Frequency Operation of DFIG based Wind Farms connected to the Grid through VSC-HVDC Link, in: Proc. 2007 IEEE PES General Meeting.

[13] I. Martinez-Sanz, Control of AC / DC Systems for Improved Transient Stability and Frequency Support Provision, Ph.D. thesis, Imperial College London, 2015.

[14] S. Akkari, J. Dai, M. Petit, X. Guillaud, Coupling between the frequency droop and the voltage droop of an AC/DC converter in an MTDC system, in: Proc. 2015 IEEE PES Eindhoven PowerTech.

[15] L. Papangelis, X. Guillaud, T. Van Cutsem, Frequency support among asynchronous AC systems through VSCs emulating power plants, in: Proc. 2015 11th IET International Conference

on AC and DC Power Transmission.
[16] J. M. Maciejowski, Predictive control: with constraints, Pearson education, 2002.
[17] S. J. Qin, T. A. Badgwell, A survey of industrial model predictive control technology, Control Engineering Practice 11 (2003) 733–764.
[18] P. McNamara, R. R. Negenborn, B. De Schutter, G. Lightbody, S. McLoone, Distributed MPC for frequency regulation in multi-terminal HVDC grids, Control Engineering Practice 46 (2016) 176–187.
[19] A. Fuchs, M. Imhof, T. Demiray, M. Morari, Stabilization of Large Power Systems Using VSC-HVDC and Model Predictive Control, IEEE Transactions on Power Delivery 29 (2014) 480–488.
[20] P. Rault, Dynamic Modeling and Control of Multi-Terminal HVDC Grids, Ph.D. thesis, Ecole Centrale de Lille, L2EP, 2014.
[21] M. Andreasson, R. Wiget, D. V. Dimarogonas, K. H. Johansson, G. Andersson, Coordinated Frequency Control through MTDC Transmission Systems, IFAC-PapersOnLine 48 (2015) 106–111.
[22] D. Jing, Y. Phulpin, A. Sarlette, D. Ernst, Voltage control in an HVDC system to share primary frequency reserves between non-synchronous areas, in: Proc. 17th Power Systems Computation Conference 2011.
[23] L. Bizumic, R. Cherkaoui, U. Hger, Ch.17 - interface Protection, in: Monitoring, Control and Protection of Interconnected Power Systems, Springer, 2014, pp. 333–347.
[24] T. M. Haileselassie, Control, Dynamics and Operation of Multi-terminal VSC-HVDC Transmission Systems, Ph.D. thesis, Norwegian University of Science and Technology, 2012.
[25] IEEE PES Task Force, Test Systems for Voltage Stability Analysis and Security Assessment, 2015. Technical Report PES-TR19, Available online on IEEE PES Resource Center. http://resourcecenter.ieee-pes.org/pes/product/technical-publications/PESTR19.
[26] P. Aristidou, D. Fabozzi, T. Van Cutsem, Dynamic Simulation of Large-Scale Power Systems Using a Parallel Schur-Complement-Based Decomposition Method, IEEE Transactions on Parallel and Distributed Systems 25 (2014) 2561–2570.
[27] P. Aristidou, L. Papangelis, X. Guillaud, T. Van Cutsem, Modular modelling of combined AC and DC systems in dynamic simulations, in: Proc. IEEE Eindhoven PowerTech.